FOCMEC: FOCal MEChanism Determinations

J. Arthur Snoke
Virginia Tech, Blacksburg, VA, USA
snoke@vt.edu

Abstract

This report accompanies a package for determining and displaying double-couple earthquake focal mechanisms. Input are polarities (P, SV, SH) and/or amplitude ratios (SV/P, SH/P, SV/SH). The main program, *Focmec* (coded in Fortran 77), performs an efficient, systematic search of the focal sphere and reports acceptable solutions based on selection criteria for the number of polarity errors and errors in amplitude ratios. The search of the focal sphere is uniform in angle, with selectable step size and bounds. The selection criteria for both polarities and amplitudes allow correction or weightings for near-nodal solutions. Published applications include determinations of best-constrained fault-plane solutions for suites of earthquakes recorded at local to regional distances (e.g., Chapman *et al.*, 1997), analysis of large earthquakes observed at teleseismic distances (Snoke, 1990), and the use of recorded polarities and relative amplitudes to produce waveform synthetics (James and Snoke, 1994).

Program *Focmec* produces two output files: a complete summary of information about all acceptable solutions, and a summary file that can be used as an input to other programs for further analysis or display. Another program in the package, *Focplt*, produces focal-sphere plots based on the *Focmec* summary file of input data (polarities and/or ratios) alone or superimposed on solutions (fault planes, compression and tension axes, SV and SH nodal surfaces). Other auxiliary programs include one to create input files for program *Focmec*, a program that converts from among various ways of presenting a double-couple solution, a program that calculates the radiation factors for an input mechanism, and programs for displaying and printing plot files. Instructions and scripts are included for compiling and running the programs, and there are two data sets with scripts and documentation for running the programs.

Earlier versions of this software package could be built and run on IBM/CMS, PDP/RSX, VAX/VMS,and Sunos. Sun Solaris, Windows 98, Linux, and Mac OS X (PPC and i686). The programs are written in Fortran 77 and compile successfully using *gfortran*, *g77*, and Sun's *f77*. Two programs written in C (*gcc*) transform graphics plot files from the Sac Graphics Format (SGF) to postscript (*sgftops*) and swap the byte order of the binary SGF files (*sgfswap*). Unix scripts (csh) are included for displaying plots on the screen and for converting plot files from postscript to EPS or PDF. The plot-conversion scripts require the external program *ghostscript*. If the user has or prefers a different postscript viewer for displaying plots, it is easy to modify the plot-display script. Except for these plot-conversion scripts, X-Windows capability is not required by the *FOCMEC* package.

I. Introduction and Overview

Given excellent station coverage for an earthquake in a region for which the earth (seismic velocity) structure was well determined, and with well recorded, impulsive P-wave first arrivals, one could get a reliable estimate for the fault-plane solution (focal mechanism) for the event. More typically, the station density is low, the velocity structure is known only approximately, and the polarities of the first arrivals are often ambiguous. For imperfect data, one may need to assume a certain number of errors to find "satisfactory" solutions, and in many cases the solutions are not well constrained. The range of possible solutions can often be further constrained if one can read, to within 10%, the P and S amplitudes on vertical-component seismograms. If one has data from three-component seismographs, the SH to P amplitude ratio provides what could be considered almost independent data. For some events, one may observe clear SH and/or SV polarities at one or more stations, and the SV/SH amplitude ratio may be better constrained than a ratio including P.

The first version of program *Focmec* was written in 1984 (Snoke, 1984), and since then advances in both seismology and computer technology have led to the introduction of routine determinations of the full moment tensor using digitally recorded waveforms (e.g., Dziewonski, *et al.*, 1981; and Sipkin, 2001). However, these techniques can generally be applied only to large earthquakes recorded at teleseismic distances or at regional distances for earthquakes large enough to have well-recorded surface waves (Randall *et al.*, 1995; Dreger *et al.*, 2000). Programs such as *Focmec* are still useful tools for getting double-couple focal mechanisms at local to regional differences, and, for the Sakhalin Island event discussed below, such programs can provide useful insights about the focal mechanism for large events using only a small number of stations.

The source code included with this distribution has been compiled and linked by the author on several Unix platforms: Sun Solaris, Mac OS X (both PPC and i686), and Linux. The coding is in *Fortran 77*, and it has been built and tested using several different compilers: *gfortran* (4.1 and 4.3), Sun *f77*, and GNU *g77*.

The *FOCMEC* software package including sources, documentation, and examples is in a compressed tar file, *focmec.tgz*. On Unix, one can uncompress and expand this file with a single command:

tar -xzf focmec.tgz

or, if has only an older version of *tar* that does not recognize -z, one can use the GNU *gtar* or a line as follows:

gzip -d -c focmec.tgz — tar -xf -

This operation produces a directory *./focmec*. Online documentation for the package can be accessed by opening the HTML file *./focmec/doc/focmec.html* and following the links to other HTML files in that directory.

To build the libraries, tables, and executables, it should suffice to go to *./src* and enter *build_package*. The default assumes the *gfortran* Fortran compiler, so if one is using a different compiler, one has to edit the first few lines of *build_package* so that it defines *FCMP*

appropriately. If the script runs with no errors, the last line displayed on the screen is a compile/link line for program *vwbeetle* (a test program for the graphics package). Executables are in directory *./bin*. To erase all executables and libraries, cd to *./src* and enter *make clean*. Scripts for testing parts of the package are in *./tests*.

The next section in this report has a discussion of the programming essentials and data preparation. The following section has a description of the programs that make up the package. The final section includes descriptions, input, and output for sample runs. Appendix A contains detailed instructions on how to prepare an input file for program *Focmec*. Appendix B contains definitions of terms used when discussing focal mechanisms. Appendix C has cautionary comments for those who want to use *SV* polarities and amplitudes, and Appendix C discusses graphics in the context of the *FOCMEC* package. README files, which contain additional details regarding running the programs, are included with the distribution in HTML format. To access the HTML files, cd to *./doc* and open *focmec.html* and follow the links. Also in *./doc* are subdirectories with the output files from scripts in the *sample_runs* subdirectories. Among the HTML files is one with an update history of the package.

II. Programming Procedure, and Data Preparation

A. Programming Procedure

The data (station identifiers, azimuths, takeoff angles at the source, polarities, and/or amplitude ratios from among *P*, *SV*, and *SH* arrivals) are read in from a file and stored. Selection parameters are entered through run-time prompts, or from user-customized script files. These include the number of allowed polarity errors for a solution, an acceptable range for deviations between the observed and calculated amplitude ratios, the number of ratio errors that are allowed to be outside that range, the region of the focal sphere to be searched, and the fineness/coarseness of the search. Using these search criteria, program *Focmec* systematically tests all possible focal mechanisms and lists those that fit the selection criteria. It stores these "possible" mechanisms in two files: a short file with one line per solution that can later be used as an input file for a plotting program, such as *Focplt*, and a more complete listing file that includes four representations of the solutions (dip, strike, rake for either possible fault plane; the **A** and **N** axes trends and plunges, the **P** and **T** trends and plunges; and the moment tensor), the station identifiers for those with a polarity error, and complete information on the calculated and theoretical amplitude ratios for each station. The conventions used are as in *Aki and Richards* (2002, pp. 101–113) and *Herrmann* (1975), except that our **A** and **N** axes correspond to Herrmann's **X** and **Y** axes. (See Snoke (1989) for a review of the terminology and conventions related to focal mechanism determinations.)

Two sets of input parameters deserve special mention: relative weighting for polarities, and, for ratios, *P* or *S* "cutoffs" when the numerator or denominator radiation factor is near a nodal surface.

1. The default polarity weighting is unity, so one gets a "1" for every modeled polarity that does not match the observed polarity. An option in the program is to use weighted polarities. Enabling this option means that a mismatch for data near a nodal surface counts less than a mismatch near the middle of the quadrant. (See Figure B3.) The weight is the theoretical radiation factor for the trial solution above a chosen threshold.

2. If the numerator or denominator radiation factor is near a nodal surface, the result is a large amplitude for the calculated $\log_{10}$(ratio). Further, the velocity structure may not be so well constrained that polarity errors near a nodal surface should be rejected. If the factor is less than the chosen cutoff, it gets replaced by the cutoff when calculating the ratio. Flags in the complete-solution output file indicate if the numerator, denominator, or both were below the cutoffs and to let the user know that those ratios may have to be examined more closely. As of the 2009 update of the package, if both the numerator and denominator are below the cutoffs (N&D), that station is rejected and the number of allowed solutions is decreased by one. For a trial solution, if the number of allowed solutions is not greater than the number of ratio errors, the solution is rejected.

B. Data Preparation

The convention for the takeoff angle is that 0° is down. The polarity convention and the notation for amplitude ratios are included in Appendix A. For phases to be used in an amplitude ratio, an implicit assumption is that the source process is simple and the travel paths similar (negligible multipathing). If the frequency content is essentially the same and the seismometers on which they are recorded are matched, one can use the raw traces. Before using *SV* data, read Appendix C below. In general, if one has 3-component data, polarities and ratios involving *SH* are more likely to be more reliable than those involving *SV*.

For calculating focal mechanisms from polarities, one needs event-based azimuths and takeoff angles for each phase from the source. If one uses amplitude ratio data, one needs the emergence angles for free surface corrections, and, if a correction for attenuation is to be used, the travel times for the phases used. These data are generally provided along with the event locations – e.g., from an earthquake-location program such as *Hypoellipse* (Lahr, 1999). If so, one could write a program (such as program *Hypo2foc* provided with this package) to take such data from the earthquake-location output file and put it directly into a *Focmec* input file. Programs *Ratio_prep* and *Focmec_prep*, also included with this package and discussed below, provide an alternative procedure to prepare a *Focmec* input file that are particularly useful if one is including amplitude-ratio data. Finally, one could simply enter the data by hand, using the *Focmec* input-file format outlined in Appendix A and by looking at the input data files included with the two sample runs (see Section IV).

For crustal events recorded at local or regional distances, the first arrivals may be the refracted phases *Pn* and *Sn*. If the Poisson's ratio is constant in the crust and uppermost mantle, *Pn* and *Sn* will leave from the same point on the focal sphere and have identical travel paths.

III. Programs

A. *Focmec*

Program *Focmec* calculates all possible focal mechanisms for an input set of polarities and amplitude ratios subject to user-specified constraints. The program requires an input file that contains the ratio and polarity data for a single earthquake. Program options can be done interactively or run from a prepared script. (Using a script is useful if one wants to test the effects of varying options for a given data set.) See the subdirectories of *./sample_runs/* for examples of both input files (called *focmecXXX.inp*) and scripts (*rfocmecYYY*). Output is two files:

1. a listing file containing detailed information about each acceptable solution (*focmec.lst*, but renamed in the script to something else to identify it with that run); and

2. an output file with a header summarizing the data and run parameters followed by a single line per solution (*focmec.out* is the default filespec). This second file can be used as input for the plotting program *Focplt* that displays data and/or solutions.

B. Other Analysis Programs

Three subsidiary analysis programs are included: *DSRetc,*, *Radiat*, and *Freesurf*. Source (.f) files are in *./src/*. No input files are required.

- *Dsretc* allows one to convert from among the various ways to represent a focal mechanism — dip, strike, rake; plunge/trend for **P** and **T** or **A** and **N**; and the moment tensor representation (for a mechanism that has a significant double-couple component). Also included is a beach-ball printer plot showing the P-wave nodal planes (Sipkin, 1993, personal communication. Sipkin gives credit to Bob Uhrhammer.)

- *Radiat* produces radiation factors and amplitude ratios for input dip, strike, rake, takeoff angle, and azimuth.

- *Freesurf* calculates free-surface corrections, which can be useful when preparing ratios input to *Focmec*.

C. *Focplt*

Program *Focplt* is the plotting program in the *FOCMEC* package. Input can be from the *Focmec* input file (for data) and/or from the *Focmec* output file (for solutions). The plots are equal-area Lambert-Schmidt projections (usually lower hemisphere) of the focal sphere. Plots can include any or all from among the following: data (polarities and/or ratios), fault planes, **P, T, B** axes, and *SV* or *SH* nodal surfaces for solutions. There are options for adding time stamps a title, and labels. The program can be run interactively or from a script. As mentioned above, programs/scripts are included that allow one to display output plot files

on the screen and to convert SGF files to postscript, EPS, and PDF. Further information on these programs and scripts is included in Appendix D.

D. Traveltime Tables

For one of the examples discussed below, takeoff angles and traveltimes are calculated using *iaspei-tau* traveltime tables. (Traveltimes are needed if one wants to do a Q correction for amplitudes.) Software for producing such tables is included in this package. As in the earlier version of this package, the *iasp91* velocity model is used (Kennett *et al.* 1991), but tables are produced here for the *ak135* model as well. The traveltime tables, which are endian and compiler dependent, are built and placed in directory *./lib/*. Files with ASCII versions of the two models are in directory *./iaspei-tau/build-tables*. Program *ttimes* is a mini-tutorial on using the traveltime tables, and *./tests/run_ttimes* is a script that does a run for that program. For more information about the *iaspei-tau* package, see Snoke (2009) and/or go to URL `http://www.iris.edu/software/downloads/processing/`.

IV. Sample Runs

Directory *./sample_runs* has two subdirectories that contain real-data applications of the *FOCMEC* package. One is for a magnitude 4.2 intraplate earthquake for which *P*-wave polarity data were collected from stations at local to regional distances. The second one is a revisit of an earlier study (Snoke, 1990): focal mechanism are calculated for a M=6.5 deep-focus (611 km) earthquake using two data sets — 190 *P*-wave polarities, and body-wave polarities as well as amplitude ratios from eight broadband stations. In the next two sections, I discuss these examples. In addition, there are HTML files for each example that can be accessed from *./doc/focmec.html*. Output listing files and plots from all the runs are included in subdirectories of directory *./doc/*.

IV A. A data set of *P*-wave polarities

Directory *./sample_runs/ETNEvent* includes drivers, and input files for an application of the *FOCMEC* package to find the focal mechanism for a magnitude 4.2 event using *P* waves recorded by 37 stations on short-period, vertical-component seismographs. The eastern Tennessee event, with a focal depth of 19 km, occurred on 27 March 1987 and is number 12 in Chapman *et al.* (1997).

The azimuths and takeoff angles for the observed *P* waves were produced by the earthquake location program *Hypoellipse* (Lahr, 1999), and the *Focmec* input file was created using program *Hypo2foc* that gets input from a *Hypoellipse* output file. The *Focmec* run with up to four unity-weighted errors had 13 solutions with very little spread. Using relative weighting for the errors produced 27 solutions with slightly more spread for a cut-off of 2.0 errors. Plots produced by program *Focplt* for the unity-weighted errors are shown in Figure 1.

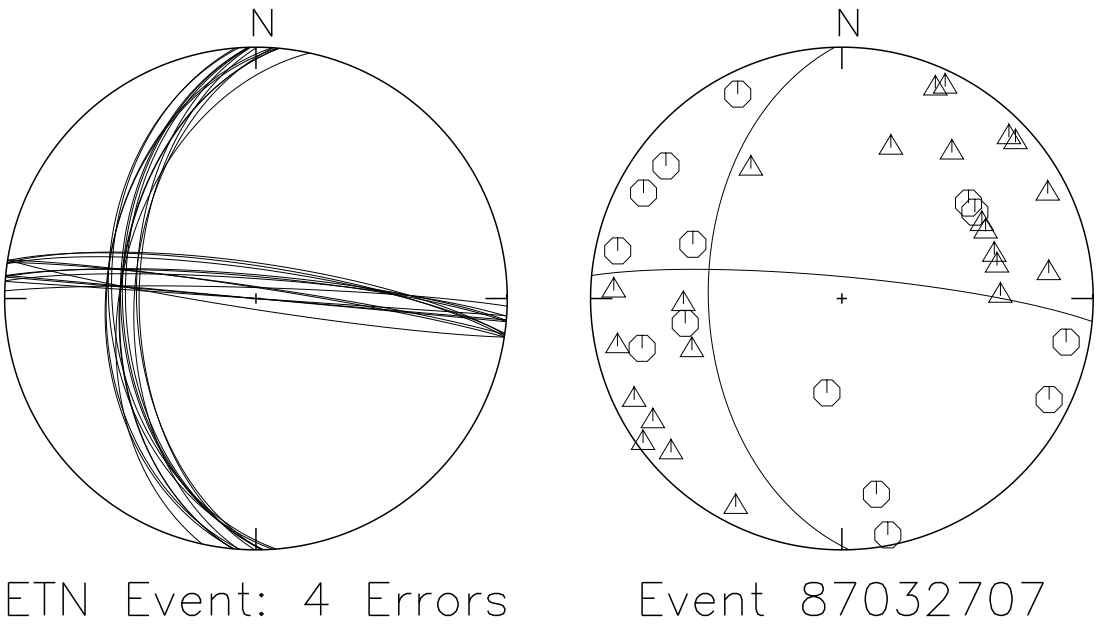

Figure 1: Lower-hemisphere projections of the focal sphere from *Focplt* runs. **(left)**: Fault planes of all solutions with four or fewer polarity errors; **(right)**: The fault planes for the acceptable solution used by Chapman *et al.* (1997) is superimposed on the polarity data. For polarities, circles represent compressions and triangles represent dilatations.

IV B. The Sakhalin Island Event: both polarities and amplitude ratios

This example includes two data sets: (1) 190 P-wave polarities, and (2) P and S polarities plus amplitude ratios from eight broadband stations. The event is the 12 May 1990 M=6.5 z=611 km Sakhalin Island earthquake. The first data set came from the NEIC within a week or two of the event. Seven of the eight broadband stations came from the IRIS DMC through their recently introduced "Gopher" quick retrieval system. The eighth broadband station was a GSETT-2 station that had been installed a few months earlier in Blacksburg (BLA) — at the observatory of my university, Virginia Tech. I used these data sets to teach myself about the quick retrieval system, the GSETT-2 station BLA, and as a test of my *FOCMEC* package. As is often the case, body-wave arrivals from this deep-focus earthquake are very impulsive — even *SV* arrivals. What is presented here is an update of my presentation at the Eastern Section of the SSA meeting (Snoke, 1990), and I include a copy of the abstract of that talk (*./doc/snoke-esssa90.pdf*). The real purpose here is to provide a worked example of the package that includes data beyond P-wave polarities, but it is also instructive because it shows that the smaller data set in this case produces a better solution. ("Better" because it differs insignificantly from the CMT solution, which includes full waveforms.) For this particular station/event geometry, the locations of some of the broadband stations to the *SV* nodal surfaces provide a significant constraint on the focal mechanism. (Figure 2).

Included in directory *./sample_runs/sakhalin* are *Focmec* runs comparing solutions based on (1) only the NEIC P-wave polarities, (2) only the broadband data, and (3) the combined data set. (The P-wave polarity from one of the broadband stations was also in the NEIC data

set.). The best solutions for (1) and (2) are significantly different, while those for (1) and (3) and the final best double-couple CMT solution are essentially the same (Figure 2).

The best fit for the NEIC P-polarity data set had 20 errors out of the 190 picks, and there were four solutions with 21 errors. (The data set includes nine emergent arrivals, but they were not included in this analysis.) Using the relative-weighting option with a threshold of 0.1 and 6.5 allowed errors produced 13 solutions that were effectively the same as the unity-weighted solutions. The unity-weighted solutions are included in the left-hand panel of Figure 2. A PDF plot from the *Focplt* run with relative weighting is included in directory *./doc/sakhalin-doc*.

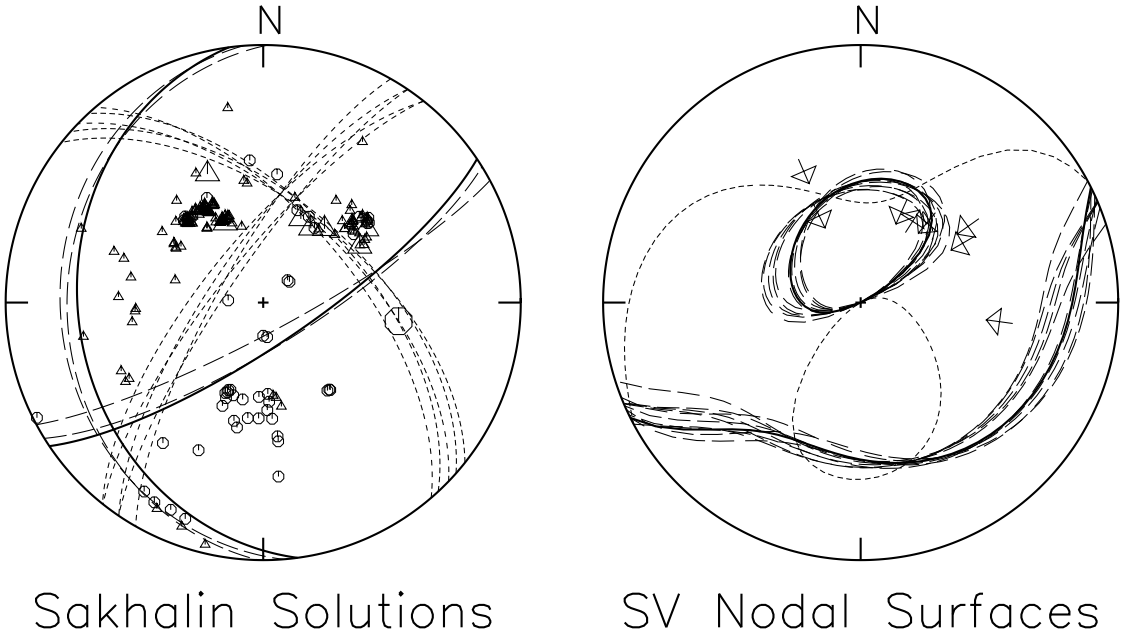

Figure 2: Lower-hemisphere projections of the focal sphere from *Focplt* runs. **(left)**: Combined data set showing all observed P-wave polarities. The eight broadband stations have larger symbols. Also shown are the fault planes for the CMT final solution (solid), composite solutions (long dashes; 27 polarity errors), and the NEIC P-polarity-only solutions (short dashes; 21 allowed errors). **(right)**: Observed SV polarities (arrows away from center $\Rightarrow$ up on the radial component) and the SV nodal surfaces for the CMT final solution (solid), all acceptable solutions for the eight broadband stations (long dashes; 0.6 SV polarity errors), .and a NEIC P-polarity-only solution (short dashes; 20 polarity errors).

Two programs were used in preparing the *Focmec* input data file for the Sakhalin Island event from the broadband stations. Program *Ratio_prep*, takes as its input a hypocenter plus a list of stations for which it calculates epicentral distances and azimuths. Using the *iasp91* velocity model and traveltime tables (Kennett and Engdahl, 1991), it calculates takeoff angles and arrival times for both P and S. The output file from *Ratio_prep*, which has one line per station, is then read by the companion program *Focmec_prep*. Program *Focmec_prep* reads in an event-specific file with one line containing the data for each polarity and/or ratio. For

polarities, the program reads in the station name and the polarity key (see Appendix A). (Emergent arrivals for which there is a polarity, can be used if desired. We chose not to use any of the nine emergent arrivals.) For a ratio, the line has the station, the ratio key, the key for the polarity of the numerator (not used, but displayed in the output listings), and either two or six numbers separated by commas — the numerator and denominator amplitudes plus (if used) attenuation data in the form Q_{num}, Q_{den}, $freq_{num}$, $freq_{den}$, where the "freq" terms are the frequencies at which the amplitudes were determined. (If an amplitude for SV is used, *Focmec_prep* assumes it is from the radial component. If the SV amplitude was measured on the vertical, it must be converted to what it would be on the radial component: program *Freesurf* can be used to calculate the conversion.) The output of *Focmec_prep* is a file that can be used as the input file for program *Focmec*.

The NEIC database and the 1990 analysis of the eight broadband stations used the *JB* velocity model and traveltime tables to calculate takeoff angles and, for the amplitude ratios, the free-surface corrections. For the runs included with this package, the *iasp91* velocity model and traveltime tables were used to allow demonstrations of programs *Ratio_prep* and *Focmec_prep*. The differences in takeoff angle are never more than a couple of degrees, which leads to negligible differences in the *Focmec* solutions. (Not done here is any fine-tuning of the free-surface corrections for individual stations, but, using the supplementary program *Freesurf*, it would be easy to modify the input for program *Focmec_prep*.)

Amplitudes used for amplitude ratios are calculated at the source. At higher frequencies, S waves lose amplitude relative to P waves because of attenuation, so if the dominant frequency is high (e.g., 1 Hz), one must correct for the relative attenuation for amplitude ratio analysis. For these data, amplitudes were measured on matched records for low-pass filtered settings with corners at 0.1 Hz (Butterworth 4 pole). Comparing the ratios with ones for which the corner was 0.01 Hz gave the same results, so no correction was used for attenuation beyond the low-pass filtering. For completeness (and to give an example of a more complicated input data file), a *Focmec_prep* run is included that has corrections for attenuation in the S/P ratios.

Because one amplitude ratio can be calculated from the other two amplitude ratios, all three are not independent. I choose the two for which the amplitudes are most easily read. When SH can be read, SH/P is generally the first choice, followed in general by SV/P.SV arrivals are picked on the radial component. (See Appendix C for a discussion about working with SV data.) For stations BLA and HRV, phase SKS arrived less than $\sim$20 seconds before direct S. If low-pass filtering is used on the radial component, SKS interferes with S resulting in a loss in accuracy for estimating the SV amplitudes. For these two stations, SV/P ratios were therefore not used. There was no interference on the unfiltered radial component, so SV/SH was used for these stations. (Q is the same for SV and SH, so one can work with the unfiltered records.)

For the analysis of the broadband data, there were 24 polarities and sixteen (independent) amplitude ratios, and in this update of the 1990 study, I corrected for the KIP and HRV polarity flips. The final *Focmec* run assumed at most 0.5 (relative weighting) SV polarity errors, zero P or SH polarity errors, and no ratio errors (with an acceptable error of 0.50 for the $\log_{10}$ ratio). This resulted in 10 acceptable solutions, which are all included in the right-hand panel of Figure 2. One can see why there might be SV nodal surfaces, as three of the stations are very near the nodal surfaces. Small changes in the location and/or velocity

models could produce small changes in the takeoff angles. This shows both that *SV* data has the potential of producing a powerful constraint, and relative weighting can be useful.

I did *Focmec* runs with the composite data sets. (As one of the broadband stations was in the NEIC data set, there was a total of only 197 *P*-wave polarities.) Assuming a total polarity error of 27, I got two solutions: one was also one in the acceptable solutions for the run with the eight broadband stations and the other would have been included in the *SV* relative error weighting threshold were 0.6 rather than 0.5. A run with 15.0 relative polarity errors included those two solutions plus three other similar solutions.

In the abstract for my 1990 presentation, I note that the composite solution was very similar to the preliminary CMT best-double-couple solution. The "final" CMT solution can be found using an event search from `http://www.globalcmt.org/CMTsearch.html`, and it is included in both panels in Figure 2. It is even closer to the composite solution than the preliminary one was in 1990.

Two more tests were made: forcing *Focmec* to accept (1) the best solution for the NEIC data set, and (2) for the CMT solution. For (1) there were 24 *P* polarities, 6 *SV* errors, and 6 *SH* errors. For ratios, *Focmec* excludes a station from the set of ratios to be considered if both the numerator and denominator are near their nodal surfaces. For this solution, this criterion dropped four from the 16 ratios. Of the remaining 12, only two were within the allowed error range. For (2), there were 14.4 *P* errors (from 29 stations) and 0.4 *SV* errors (from three stations). No *SH* polarity or ratio errors, and none of the *P* errors were from among the broadband stations. If the grid search in *Focmec* had included this solution, it would have been found to be acceptable in either the broadband analysis or the relative-weighting composite data analysis. There is a discussion in the HTML file about how to do a *Focmec* run to a fixed location on the focal sphere when that solution was not generated from an existing *Focmec* run.

The seismograms for KEV (at 54.58°) show numerous body-wave arrivals in addition to direct *P* and *S*. The *iasp91* package gives arrival times and takeoff angles for (almost) all these phases, so in principle, these polarities could be used as additional input to program *Focmec* — after allowing for any polarity flips on reflection or conversion. If such arrivals are well recorded, one could use amplitude ratios from among them (but one would have to include conversion/reflection coefficients). However, in this particular case, one arrival is probably not the one predicted by the *iaspei-tau* package, so care must be taken. A figure showing the KEV seismograms and a discussion are included in a PDF file *./doc/sakhalin-doc/KEV_phases.pdf* refracted from Snoke(2009).

V. References

Aki, K. and P. G. Richards (2002). **Quantitative Seismology: Theory and Methods**, W.H. Freeman, San Francisco, CA, Second edition.

Booth, D. C. and S. Crampin (1985). Shear-wave polarizations on a curved wavefront at an isotropic free surface, *Geophys. J. R. astr. Soc.*, **83**, 31–35.

Chapman, M. C., C. A. Powell, G. Vlahovic and M. S. Sibol (1997). A statistical analysis of earthquake focal mechanisms and epicenter locations in the eastern Tennessee seismic zone, *Bull. Seism. Soc. Am.*, **87**, 1522–1536.

Dreger, D. S., H. Tkalĉić, M. Johnston (2000). Dilational processes accompanying earthquakes in the Long Valley Caldera, *Science*, **288**, 122–125.

Dziewonski, A. M., T. A. Chou, and J. H. Woodhouse (1981). Determination of earthquake source parameters from waveform data for studies of regional and global seismicity, *J. Geophys. Res.*, **86**, 2825–2852.

Goldstein, P., D. Dodge, M. Firpo, and. S. Ruppert (1998), What's new in SAC2000? Enhanced Processing and Database Access, *Seism. Res. Letters*, **69**, 202–204

Gubbins, D. (1990). **Seismology and Plate Tectonics**, Cambridge University Press, Cambridge

Herrmann, R. B. (1975). A student's guide for the use of P and S wave data for focal mechanism determination, *Earthquake Notes*, **46/4**, 29–39.

James, D. E. and J. A. Snoke (1994). Structure and tectonics in the region of flat subduction beneath central Peru. Part I: Crust and uppermost mantle: *J. Geophys. Res.*, **99**, 6899–6912.

Jost, M. L. and R. B. Herrmann (1989), A student's guide to and review of moment tensors, *Earthquake Notes*, **60/2**, 37–57.

Kennett, B. L. N., and E. R. Engdahl (1991). Traveltimes for global earthquake location and phase identification, *Geophys. J. Int.* **122**, 429–465. Source code for building the tables for both *iasp91* and *ak135* can be gotten from URL `http://www.iris.edu/pub/programs/iaspei-t`

Kisslinger, C. (1980). Applications of S to P amplitude ratios for determining focal mechanisms from regional network observations, *Bull. Seism. Soc. Am.*, **70**, 999–1014.

Kisslinger, C., J. R. Bowman, and K. Koch (1981). Procedures for computing focal mechanisms from local (SV/P) ratios, *Bull. Seism. Soc. Am.*, **71**, 1718–1729. Correction for both this and the preceding paper was published in *BSSA* volume **72** on page 344.

Kisslinger, C., J. R. Bowman, and K. Koch (1982). Determination of focal mechanisms from (SV/P) amplitude ratios at small distances, *Phys. Earth and Planet. Inter.*, **30**, 172–176.

Lahr, J. C. (1999), HYPOELLIPSE Y2K: A computer program for determining local earthquake hypocentral parameters, magnitude, and first-motion pattern, U.S. Geological Survey Open-file Report 99–023, 112p. On-line: http://greenwood.cr.usgs.gov/pub/open-file-reports/ofr-99-0023. http://geohazards.cr.usgs.gov/iaspei_pgms/hypoellipse/ is the URL for the current version of the package, including documentation and executables for both PC and Sun/Unix.

Randall, G. R., C. J. Ammon and T. J. Owens (1995). Moment-tensor estimation using regional seismograms from a Tibetan Plateau portable network deployment, *Geophys. Res. Letters*, **22**, 1665–1668.

Sipkin, S. A. (2001). USGS Moment tensor software and catalog, this volume.

Snoke, J. A., J. W. Munsey, A. C. Teague, and G. A. Bollinger (1984), A program for focal mechanism determination by combined use of polarity and SV-P amplitude ratio data, *Earthquake Notes*, **55, #3**, 15.

Snoke, J.A. (1989). Earthquake Mechanisms, **Encyclopedia of Geophysics** (D. E. James, Ed.), Van Nostrand Reinhold Company, New York, 239–245.

Snoke, J.A. (1990), Clyde and the Gopher: a preliminary analysis of the 12 May 1990 Sakhalin Island event, Eastern Section of the SSA meeting (Blacksburg, VA, October), *Seism. Res. Letters*, **61**, 161.

Snoke, J.A. (2009), Traveltime Tables for iasp91 and ak135, *Seism. Res. Letters*, **80(2)**, 260–262.

Stein, S. and E. Klosko (2002), Earthquake Mechanisms and Plate Tectonics, **International Handbook of Earthquake and Engineering Seismology** (W. H. K. Lee, H. Kanamori, P. C. Jennings, and C. Kisslinger, Eds.), Academic Press, San Diego, Chapter 7.

Appendix A: Input conventions and format for *Focmec* and *Focplt*

This is a text file describing the input format for *Focmec* (done in subroutine focinp.f) and which is used in program *Focplt* (through subroutine *prplot.f*) for displaying first motions and/or ratios.

```
        READ(1,'(A)') COMMNT !  First line input file
200     READ(1,5,END=300,ERR=500) STA,AZIN,TOANG,SENSE,
     .     RATLOG,SVSH2,STOANG,INFO
5       FORMAT(A4,2F8.2,A1,F8.4,1X,A1,1X,F6.2,1X,A)
```

- STA is a name for the station. Up to four characters. Not used
- AZIN is the azimuth (degrees) of the station measured from the epicenter
- TOANG is the takeoff angle (degrees) of the S if S polarity or a SV/P, SH/P, or SV/SH ratio. It is a P takeoff angle for a P polarity
- SENSE is a one-character key for a polarity or a ratio

```
Virginia Tech Symbol conventions:
  C = compression at station (plotted as a hexagon symbol number NS = 1)
  U = same as C (up on vertical)
  D = dilatation --- down on vertical (plotted as a triangle NS=2)
  + = emergent compression  (NS=3) (optionally included in Focmec)
  - = emergent dilatation  (optionally included in Focmec
  e = emergent P arrival
  > = SH first motion to right (back to event, facing station) impulsive
  < = SH first motion to left (back to event, facing station) impulsive
  L = same as <
  R = same as > (Note: earlier versions used R for SV/P ratio)
  F = SV first motion away from event impulsive
  B = SV first motion towards event impulsive
    The SH and SV first motions are plotted as oriented arrows (NS=6)
  l = SH first motion to left (back to event) emergent
  r = SH first motion to right (back to event) emergent
  u = emergent SH arrival
  V = Log10(SV/P)  (NS=4) (plotted as an X)
  H = Log10(SH/P)  (NS=4) (plotted as an X)
  S = Log10(SV/SH) (NS=4) (plotted as an X)
```

If one wants to have errors marked, follow the polarity or ratio with a duplicate line with an E in the symbol position. The error will then be flagged by a square superimposed on the polarity or ratio. If SENSE is R, V, or H:

- RATLOG is the $\log_{10}$ (S/P)

- SVSH2 is the polarity of numerator S. It is not used, but is shown in the listing file along with the calculated values. Convention used for the calculated ones are L and R for SH, B and F for SV
- TOANG1 is the S takeoff angle
- INFO is a field of up to 40 characters. If the input file was prepared by Focmec_prep, it summarizes information used in the amplitude ratio. (See *./sample_runs/sakhalin* for an example.)

No terminator line is needed. MAX in FOCMEC.INC is the maximum number of allowed ratios plus polarities.

Appendix B: Glossary for Focal Mechanisms

Seismic Moment Tensor: The ground displacement from an earthquake can be written as the convolution of a moment tensor and the gradient of a Green's function. The Green's function includes propagation effects, while the moment tensor contains information about the source properties. The moment tensor can be interpreted as the volume integral of the stress release associated with the earthquake. The most general moment tensor has six independent components, but the focal mechanisms for the vast majority of earthquakes are well described by a *double couple*, for which the moment tensor has only three independent components. See Jost & Herrmann (1989) for a comprehensive review of moment tensors.

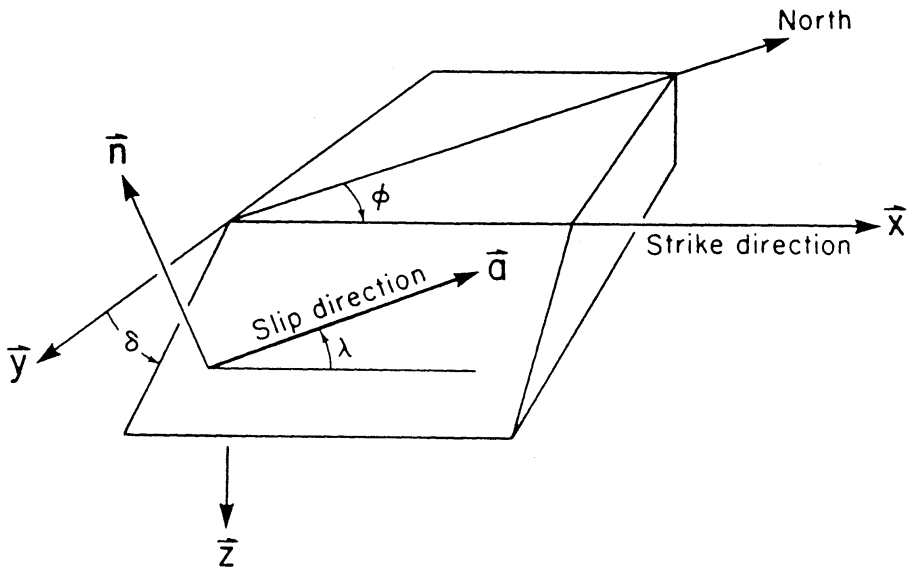

Figure B1: Schematic of the *foot-wall* side of a fault showing the conventions for the fault parameters: strike (ϕ), dip (δ), rake (λ), and slip direction ($\vec{a}$). The normal to the fault is $\vec{n}$. (After Snoke, 1989, Figure 2, which was in turn adapted from Aki and Richards, 2002, Fig. 4.13.)

Strike, Dip and Rake: One way to parameterize a double-couple solution is to specify, with three angles, the direction of a vector along the direction of slip of the earthquake along a fault surface. The **strike** (ϕ) is the azimuth of the fault, with the convention that if one faces down-dip, the strike direction is to the left. The **dip** (δ) is measured down from the horizontal and is bounded by 0° and 90°. The **rake** (λ) is along the direction of slip on the fault surface and is bounded by –180° and +180°. The convention for rake angle λ: Reverse fault if $0° < \lambda < 180°$, normal fault if $-180° < \lambda < 0°$, right-lateral strike slip if $\lambda = 180°$, and left-lateral strike slip if $\lambda = 0°$. Note that with $\hat{z}$ down (Figure B1), both ($\hat{x}$, $\hat{y}$, $\hat{z}$) and (North, East, $\hat{z}$) are right-handed coordinate frames.

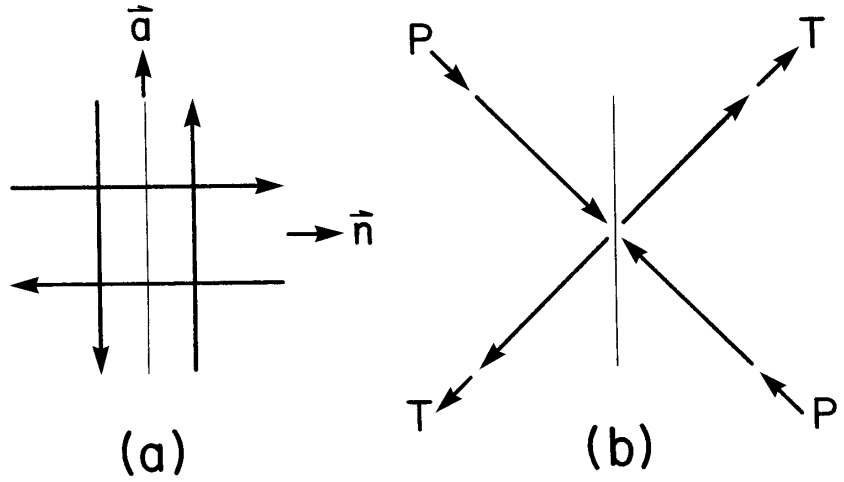

Figure B2: Two representations of the double-couple point-source model for strike-slip motion on a vertical fault. **(a)** moment tensor is evaluated in a coordinate frame such that $\hat{x}_1$ lies along $\vec{a}$. the slip direction, and $\hat{x}_2$ along $\vec{n}$, the normal to the fault plane. (Direction $\hat{x}_3$ is into the page.) **(b)** normal forces corresponding to the same moment tensor in a coordinate frame rotated clockwise from the one in **(a)** By 45° about $\hat{x}_3$. **T** is the tension axis, and **P** the compression axis. (After Snoke, 1989, Figure 3.)

Pressure and Tension Axes: As shown in Figure B2, an alternative parameterization for a focal mechanism is to specify the trend and plunge of the **P** axis (direction of maximum source compression that is the same as the direction of maximum dilatation at the recording site) and **T** axis (direction of maximum source dilatation or recording-site compression). Because the **P** and **T** axes are orthogonal, there are only three independent parameters from among the two sets of trends and plunges, so there are still only three independent parameters in this representation. This representation for a focal mechanism is particularly useful for relating earthquake mechanisms to directions of compression or tension of the regional stress.

Focal Sphere: Modeling the earthquake as a point source, the focal mechanism can be uniquely specified by specifying the directions of **P** and **T** with respect to a sphere of vanishingly small radius surround the focus (Figure B2b). Observations of polarities and amplitudes used to constrain the solution must be corrected to points on the focal sphere designated by the takeoff angle and azimuth for the raypath leading to that station.

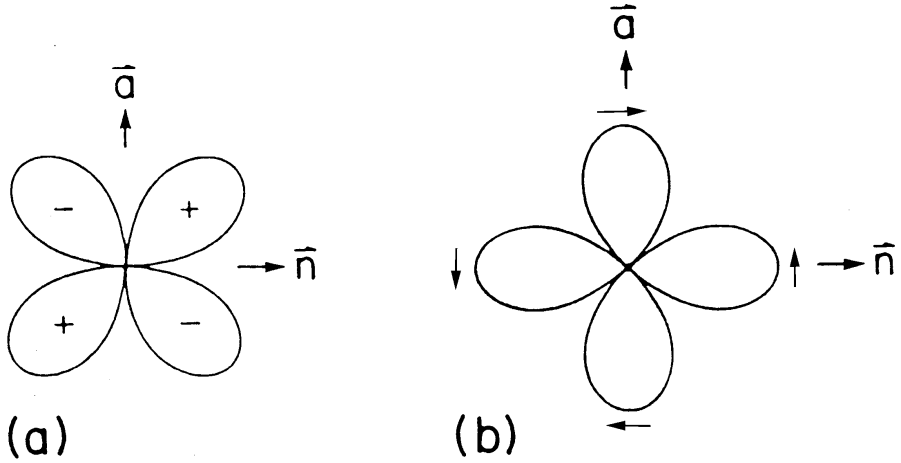

Figure B3: Radiation patterns for **(a)** P waves and **(b)** SH waves for a vertical strike-slip fault oriented as in the previous figure. In **(a)** the + and – indicate the direction of first motion of the P with respect to the source, and the arrows in **(b)** indicate the first-motion directions for SH. (After Snoke, 1989, Figure 1 — except the direction of the SH polarity arrows have been reversed from that figure)

Radiation Pattern: A double-couple solution produces a radiation pattern for P waves with four quadrants that are alternatively compressive and dilatational. Figure B3 shows the four quadrants for both the P and SH radiation patterns.

Fault Plane and Auxiliary Fault Plane: The radiation patterns for SV and SH have similar four-fold symmetry to that for P, and the result is that there are two equally possible fault planes consistent with all polarity and ratio data for a single event. Hence for each solution, two possible sets of dip, strike and rake are presented, and each fault-plane plot includes two planes. Solutions produced by program *Focmec* include the trend and plunge of vectors **A** and **N**, which are along the slip directions in the two possible fault planes ($\vec{a}$ and $\vec{n}$ in the preceding two figures in this section). These vectors can be gotten from **P** and **T** by a rotation of 45° around the vector **B**, which is along the normal to the plane formed by **P** and **T**.

Sign Conventions for Components of Ground Motion: Polarities in the FOCMEC package are designated by directions with respect to an observer facing the station with his/her back to the epicenter. Accordingly, P arrival first motions are up or down, SH left or right, and SV forward or backward.

Horizontal components for a three-component seismograph must be rotated from *North-South* and *East-West* into *Radial* and *Transverse* to separate SV from SH. The convention in common usage — e.g., in SAC — has positive Radial as forward and positive Transverse as to the right with respect to an observer facing the station. Note that *Vertical*, *Radial*, and *Transverse* form a left-handed coordinate frame.

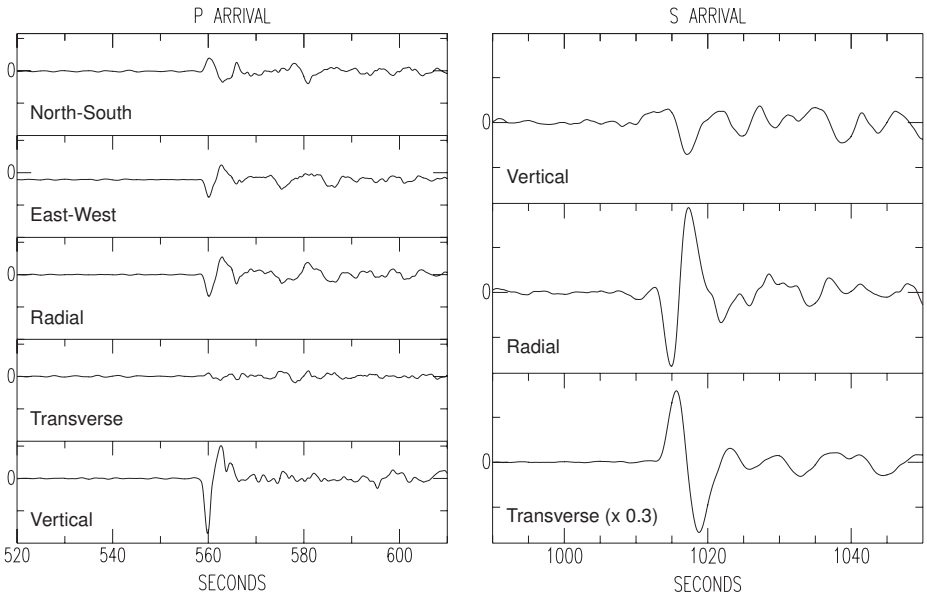

Figure B4: Components for P (left) and S (right) arrivals at station COR for the Sakhalin Island event. The backazimuth is 311°, so the direct arrivals come from the northwest. Positive for the Radial component is hence towards the southeast, and positive on the Transverse is towards the southwest. For display purposes, the P arrivals are lowpass filtered and S on the transverse component is rescaled.

From Figure B4, one can see the basis for the polarity choices for station COR in the *focmec* input files in subdirectory ./sample_runs/sakhalin: D (down on Vertical) for P, B (down on Radial) for SV, and R (up on Transverse) for SH.

Upper- and Lower-Hemisphere Projections: The projections of the focal spheres shown above in Figures 1 and 2 are lower-hemisphere projections. This is the more popular projection, presumably because most data are teleseismically recorded. Some times an upper-hemisphere projection is used, so it is instructive to review briefly how these projections are related and how one constructs them.

The particle motion is identical for antipodal points on the focal sphere, so a projection (from above) of station positions and focal mechanism onto the upper hemisphere can be mapped onto the lower hemisphere by simply adding 180° to all station azimuths and trends for the **P** and **T** axes.

To get such plots, one projects the position on the focal sphere of the **P** and **T** axes (trends and plunges) and station polarities or amplitude ratios (takeoff angles and azimuths) onto a circle. For a station position, if it is an upper-hemisphere projection and the takeoff angle is up, the mapping is straightforward. If for that projection the takeoff angle is down, one maps the antipodal position onto the circle — the supplement of the takeoff angle and azimuth plus 180°. For a lower-hemisphere projection, the mapping is the opposite. It is easiest to derive the nodal surfaces from the directions of the **P** and **T** axes: As these axes project in antipodal directions from the focus, to map a lower-hemisphere vector into its upper-hemisphere counterpart, one simply adds 180° to the trend.

"Beachball" Representations of Focal Mechanisms

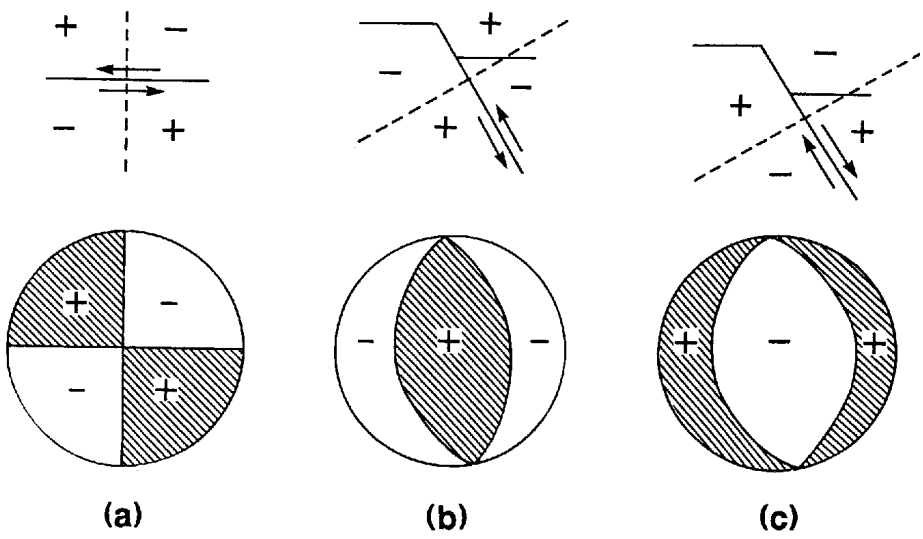

Figure B5: Shown are *beachball* representations of the P-wave radiation pattern for the three fundamental double-couple fault types: **(a)**: pure strike-slip faulting, **(b)**: pure dip-slip reverse (thrust) faulting, and **(c)**: pure dip-slip normal faulting. Above each is a sketch of the fault geometry for that mode of faulting. (The auxiliary plane is shown as a dashed line.) The compressional quadrants are shaded, and the sign of the direction of vertical-component first motion is included for each quadrant. (Usually these signs are not included.) Such plots are an efficient method to show trends in focal mechanisms for groups of earthquakes. See, for example, figures in the paper by Stein & Klosko, 2002. Such plots are also used to represent non double-couple mechanisms with nodal-plane projections replaced by nodal-surface projections. (After Gubbins, 1990, Figure 6.7.)

Appendix C: SV Polarities and Amplitudes Should be Used with Care

Kisslinger and coauthors (1980, 1981, 1982) describe procedures for using SV/P vertical-component amplitude ratios recorded by local and regional networks to constrain focal mechanisms. The emphasis was on the vertical components because at that time most networks used single-component seismographs and analog recording.

With modern instrumentation, one can often find well recorded SV arrivals — although generally not as well recorded as for the deep-focus Sakhalin Island event discussed above. We show below why SV should be used only with great care.

Figure C1: Ray geometries showing directions of positive first-motions for free-surface incidence of P (left) and SV (right). This conventions differs from that used by Aki & Richards (2002, Figure 5.5) only for the direction of incident SV. I use this convention because for both P incidence and SV incidence, there is the same relationship between propagation directions and particle motion for incoming and reflected rays.

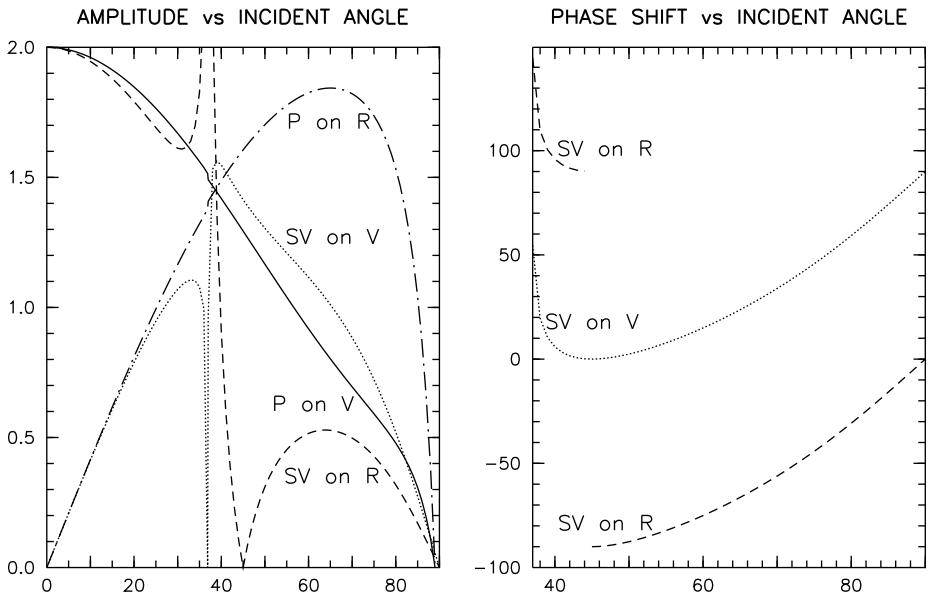

Figure C2: Free-surface amplitudes (left) and phase shift (right) for emergent P and SV at the free surface for a v_S/v_P ratio of 0.6. The critical angle is $\sin^{-1}(v_S/v_P) = 36.9°$.

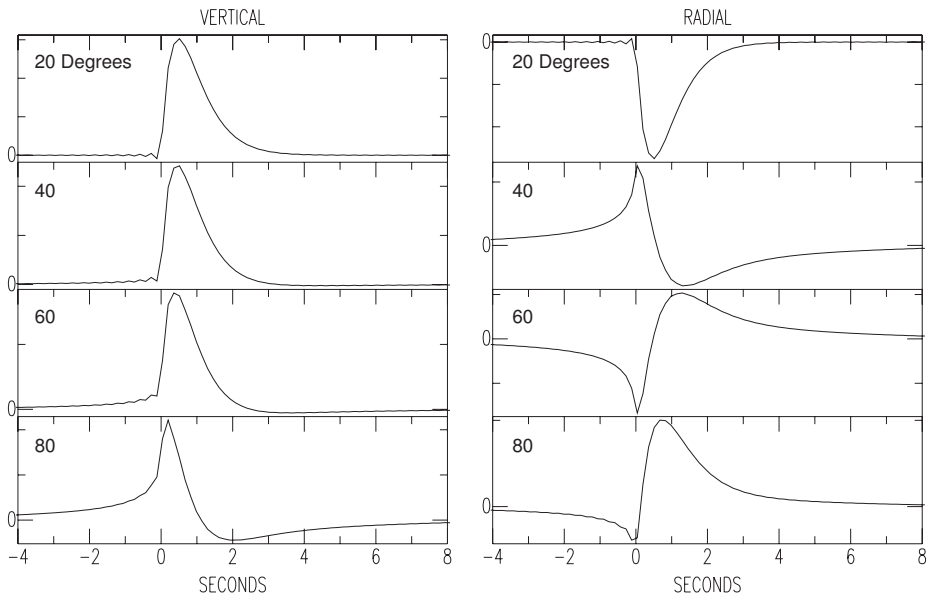

Figure C3: Waveforms for the vertical ground motion (left) and the radial ground motion (right) for plane wave SV incidence angles of 20, 40, 60, and 80 degrees in a uniform halfspace with a v_S/v_P ratio of 0.6. Polarities follow the convention defined in Figure C1.

The input waveform for the ground motion shown in Figure C3 is normalized so that the area under the curve is the same as the amplitude for that component shown in Figure C2 when there is no phase shift. For P incidence, there is no critical angle and the polarities are all positive using the convention defined in Figure C1, so there is zero phase shift for all angles of incidence. The rest of this discussion is for SV incidence.

As discussed by Aki & Richards (2002, page 151), the sign of the "phase shift" depends on the Fourier sign convention and on the sign of the frequency. The phase shifts in Figure C2 use their conventions: positive frequencies and $+i\omega t$ for the forward Fourier transform. Because of the different polarity for SV incidence between them and Figure C1, phase shifts presented here will differ by 180° from theirs.

Below critical angle incidence, the phase shift is zero for the vertical ground motion and 180° for the radial motion (see waveforms for 20° incidence in Figure C3). At 45° incidence, the phase shift for the radial component jumps by 180°, which can be seen in the polarity flip between the waveforms on the radial component for 40° and 60° in Figure C3.

The rapid changes in amplitude within a few degrees of the critical angle mean that neither the vertical nor radial component amplitudes should be used for arrivals at those angles.

One sees from Figure B4 above that for small emergence angles (22° at COR for S for this event), SV is much better recorded on the radial than the vertical. In general, below about 30° SV on the radial component is the more reliable. For angles above the critical angle, the phase shift results in a drastic change in waveform for the radial component, so SV on the radial should definitely not be used in ratios and used only with great care for polarity.

For the vertical component with SV incidence, the polarity is stable up to about 80°, so those polarities can be used if the arrivals are well recorded. Up to about 50°, the small phase shift results in a negligible change in the amplitude, so the vertical component could be used in an amplitude ratio. At 80°, the waveform shown in Figure C3 is visibly changed and the amplitude is reduced to $0.27/0.52 = 0.52$ the amplitude predicted by the free-surface correction plotted in Figure C2.

Kisslinger *et al.* (1961) write that the free-surface correction for the SV/P ratio on the vertical, the free-surface correction is close to unity for incidence angles from a few degrees above the critical angle to about 80°. While that is true based on the amplitudes shown in Figure C2 (see also their Figure 1), the effect of the phase shifts on the waveforms and amplitudes leads to a much larger variation for higher angles.

The above discussion is based on plane wave incidence — appropriate for teleseismically recorded events. In their paper on shear-wave polarization, Booth & Crampin (1985) show that for curved wavefronts associated with local to near-regional events, an SP arrival that comes in just before direct S affects the observed waveforms. In addition, a low-velocity zone at the surface can complicate the waveforms — particularly for SV incidence. Such considerations must also be considered when choosing polarities and amplitudes for focal mechanism determinations.

Appendix D: Graphics in the FOCMEC package

As described above, program *Focplt* produces plots of focal-sphere projections of data and/or fault-plane solutions. Earlier versions of the *FOCMEC* package used the SAC (Goldstein, *et al.* 1998) Fortran library that was distributed with pre-1994 versions of SAC. This library allowed the user to create both plot files and interactive on-screen plots. The screen-plot option has been dropped, because the 15-year old libraries were obsolete. Program *Focplt* continues to use the SAC Graphics Format (SGF) to produce disk files. Program *sgftops* converts .sgf files to postscript files. The *FOCMEC* package can be compiled and run on "big-endian" systems (Sun Solaris, Mac OSX PPC) or "little-endian" systems (Linux, Mac OSX i686/intel) that have the opposite byte order for binary data. Because a .sgf file is a binary file, program *sgftops* will only work on a .sgf file that has one byte order. If there is a byte-order mismatch, *sgftops* will exit with the message that one should run program *sgfswap* on the file. Program *sgfswap* is provided with the package.

Also included are four (Unix csh) scripts:

1. *plsgf*: produces a print of a .sgf file.

2. *sgftox*: Displays a .sgf plot on the screen. As written, the script uses program *gs* (*ghostscript*), but one can substitute a different postscript-file display program.

3. *sgftoeps*: produces a EPS file (Encapsulated Postscript file) from a .sgf file. Program *gs* is required.

4. *sgftopdf*: produces a PDF file from a .sgf file. Program *gs* and the Perl script *epstopdf* are required.

To find out more the programs or scripts, enter the program or script name with no arguments.

The file *./doc/graphics.html* has more information about how to test the graphics package and how one can use the symbol routine to label plots.

Several scripts in Section IV run program *Focplt* to produce SGF files. Note that those for the Sakhalin Island event superimpose sets of solutions, so studying them may be helpful regarding how one answers the prompts for adding additional solutions. The screen output for these scripts is ported into a file named *a.junk* in the same directory, so if the script exits with an error message, comparing the contents of that file with the calling script should help the user find the error.

The scripts have calls to *sgftox* and it sgftopdf, and the PDF plots are included in the *./doc* subdirectories for each application. The figures in this document were produced from SGF plots using *sgftoeps*.